A New Perspective of the Glass Transition of Polymer Single-Chain Nanoglobules

Yongli Mi,*,† Gi Xue,†,‡ and Xiaolin Lu†

Department of Chemical Engineering, Hong Kong University of Science and Technology, Clear Water Bay, Kowloon, Hong Kong, and Department of Polymer Science, Nanjing University, Nanjing, China

Received February 20, 2003; Revised Manuscript Received July 21, 2003

ABSTRACT: The glass transition behavior of polyacrylamide (PAL) was investigated in the bulk entangled state, the single-chain isolated state, and the partially entangled state. It was observed that the glass transition temperature increases as the degree of entanglement decreases. Single-chain nanoglobules of PAL were prepared by spray drying and the partially entangled PAL sample was prepared by freeze-drying from solutions of different concentrations. The glass transition temperature (T_g) was measured by using differential scanning calorimetry (DSC). The enthalpy relaxation peak of the single-chain nanoglobules was found to be sharper and higher than that of the bulk PAL, whereas the partially entangled PAL exhibited two enthalpy relaxation peaks. The cohesional entanglement theory is adopted in the discussion. The DSC results of this study appear to be consistent with the concept of cohesional entanglement. It was also found that, at the same annealing condition, the single-chain PAL globules have much higher T_g than that of the bulk PAL. The single chains, after spray-drying, are in the form of loose chain coils; upon thermal treatment, the chain coil becomes more compact. The bulk polymer also shows the same trend, but due to the entanglement in the bulk polymer, the increase in T_g is smaller compared to the T_g increase for single-chain globules.

Introduction

Although the glass transition is a well-known phenomenon for liquids with strong covalently bonded structures, and is especially noteworthy for amorphous polymers, understanding the glass transition still remains one of the most intriguing puzzles in condensed matter physics at present. The solution of the glass transition puzzle will ultimately influence different fields, particularly biophysics and biochemistry.[1]

Due to the high degree of interchain entanglement in polymers, a theoretical approach to the glass transition of polymers is hindered by a series of metastable states in bulk polymers. Therefore, a true equilibrium state can never be approached in amorphous polymers below the glass transition temperature. For a better understanding of the complicated problem, there have been reports discussing the glass transition of polymers in confined geometries.[2−20] One of the approaches is to examine the glass transition of polymer thin films. The glass transition temperature (T_g) in thin film geometry, as measured by spectroscopic ellipsometry, X-ray reflectivity, and Brillouin scattering, depends on the film thickness and the molecular weight of the polymer.[2−13] In particular, the measurement of a free-standing polystyrene film has indicated a 70 °C decrease in the effective T_g when film thicknesses approached tens of nanometers.[9] There have been different arguments proposed to explain this decrease, including the enhanced mobility of surface layers,[7,9] a decrease in the film density,[14] a decrease in the entanglement,[15] an enrichment of chain ends on the surface,[16,17] and the sliding-loop dynamics of De Gennes.[18] However, the effect of thin film geometry can also be interpreted in terms of a second-order transition, because, in Ising models,[20,21] the critical temperature in two dimensions is lower than its corresponding value in three dimensions. Since the thin film puzzle could be simply a quasi-two-dimensional problem, a test on a nanosized three-dimensional particle will shed light on the problem.

In a previous study, we presented a case in which polymer chains were confined in three-dimensional nanosized globules, and we observed a significantly higher T_g for polyacrylamide (PAL) in the single-chain globular state than that in the bulk state.[22] Our results were clearly not in agreement with those reported for thin films[2−13] and proposed by kinetic theories.[7−9,14−18] In this study, we present more experimental details and systematically evaluate the glass transition behavior in the entangled bulk state and in the isolated single-chain globular state.

Experimental Section

Materials. PAL with a molecular weight of MW = 5000000 was ordered from Polysciences, Inc., Warrington, PA. An aqueous solution of 10^{-4} wt % was prepared for spray-drying.

Spray-Drying. A Mobile Minor Basic Model Niro spray-dryer was purchased from Niro, Gladsaxevej 305, DK-2860 Soeborg, Denmark. A diagram of the spray-dryer and of the auxiliary components is shown in Figure 1. The spray-dryer consists of the following units: (A) a polymer solution feed from a rotary pump, (B) a roof air disperser which ensures effective control of the air flow pattern (processed swirling hot air is directed around the atomizer), (C) a rotary atomizer, (D) stainless steel interconnecting pipes, (E) an air valve for activation of the pneumatic lifting device to raise the chamber roof, (F) the sample collecting unit in which the powder and the exhausted air are separated in a highly efficient stainless steel cyclon, (E) the sample bottle in which the powder is collected under the cyclon, (H) the instrument panel with operating switches for the fan, electric air heater, and feed pump, a digital controller for the inlet air temperature, a digital indicator for the outlet air temperature, and a valve and pressure gauge for speed regulation of the atomizer wheel,

* To whom correspondence should be addressed. E-mail: keymix@ust.hk. Phone: (852) 2358-7127.
† Hong Kong University of Science and Technology.
‡ Nanjing University.

10.1021/ma030127j CCC: $25.00
Published on Web 09/13/2003

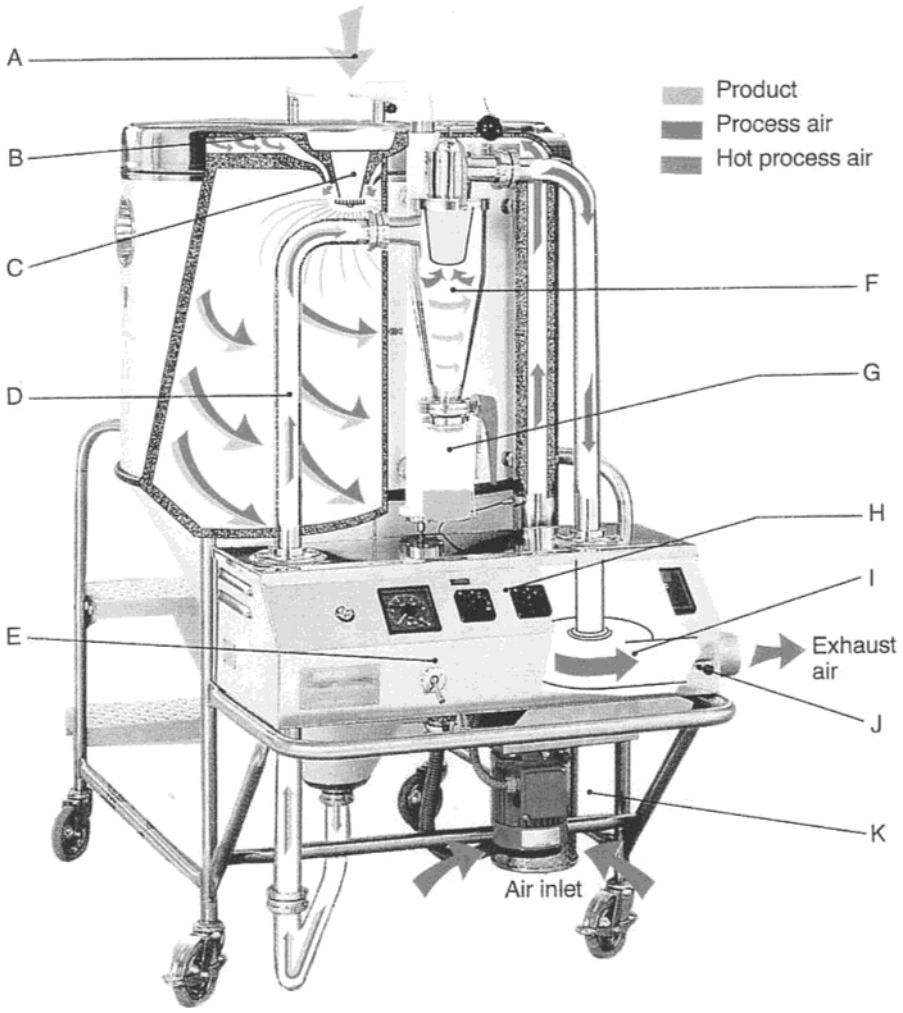

Figure 1. Diagram of the spray-dryer and of its auxiliary components.

(I) a centrifugal exhaust fan with a three-phase motor, (J) a damper for air flow control, and (K) a 7.5 kW electric air heater that heats the process air. The air temperature can be continuously adjusted. In this study, the inlet temperature was 170 °C, the chamber temperature was 100°C, and the outlet temperature was 90 °C.

Freeze-Drying. Freeze-dried PAL samples were also used for the study of the effect of entanglement on the glass transition. The freeze-dried PAL samples were prepared by dissolving the desired amount of the original PAL in distilled water with varying concentrations. The solution was injected directly into liquid nitrogen for shock-cooling so that they were frozen in a fraction of a second. The frozen water was sublimated at −50 °C under high vacuum for one week and then kept under vacuum at room temperature for another 3 days to remove possible residual solvents.

Differential Scanning Calorimeter. The differential scanning calorimetry (DSC) measurement was performed using a Perkin-Elmer-7 DSC apparatus. Before the measurement, the temperature calibration was done with standard indium and Zn. The standards were supplied by the Perkin-Elmer Co. For every DSC measurement, the weights of the sample pan with cover and the reference pan with cover were matched by carefully pairing the pan and the cover using a microbalance. A DSC curve with two empty pans was recorded as a baseline. After a DSC curve of a sample was recorded, the baseline was subtracted from the DSC curve, which is called baseline correction. All samples were subjected to drying in a vacuum oven for 6 days at 60 °C.

Transmission Electron Microscope. The transmission electron microscope, Philips CM 20, was operated at 200 kV to examine the size of single-chain particles.

Ultramicrotome. A Leica Ultracut R ultramicrotome with an EM FCR low-temperature sectioning system was used to prepare the TEM specimens. The cutting temperature was −120 °C in liquid nitrogen, the cutting speed was 0.5 mm/s, and the specimen thickness was 70 nm.

Results and Discussion

State-of-the-Art Sample Preparation. The polymer solution of 10^{-4} wt % was fed through a rotary pump to the spray-dryer and atomized. The polymer powders were collected at the sample bottle (G) (Figure 1). The powder was dried in a vacuum oven at 50 °C for 48 h. Figure 2 shows the SEM photo of the PAL powder as collected from the sample bottle (G). The SEM results indicate that the particle size of the spray-dried sample was in the range of 1−4 μm. In our previous study, we demonstrated that, by adopting this conventional spray-drying method, we could attain isolated single-chain particles.[23] Our original postulation was that, by letting the liquid droplet, which contains many polymer molecules in the isolated single-chain state, evaporate very quickly, the chain entanglement within the droplet could be prohibited due to the fast evaporation rate, so that the single-chain particles could be obtained efficiently. The spray-dryer can cause the droplet to be dried in milliseconds. We then used TEM to examine the internal structure of the micrometer particles obtained from the spray-drying.

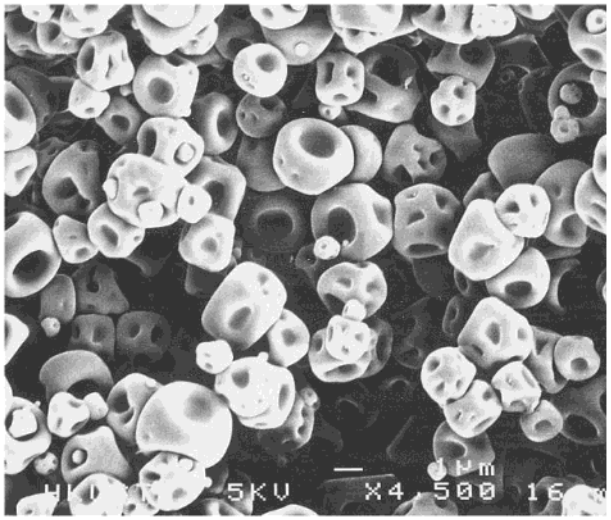

Figure 2. SEM photo of the PAL powder collected after spray-drying.

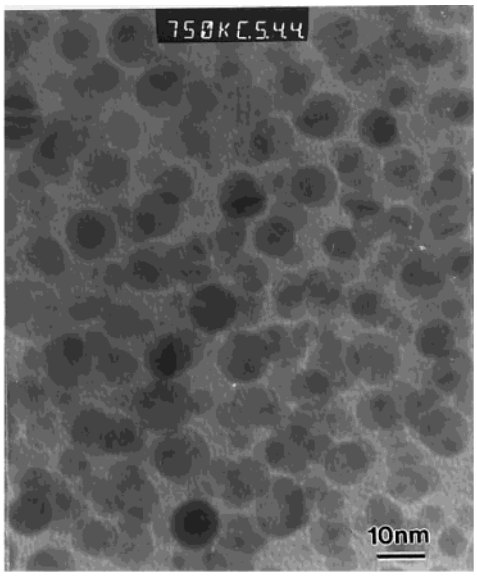

Figure 3. TEM image of the single-chain PAL nanoglobules.

To obtain thin films for the TEM studies, the micrometer particles from the spray-drying were fixed in epoxy, EPO-TEK 301, purchased from Epoxy Technology, Inc., Billerica, MA. The weight ratio of the epoxy and the curing agent was 10:3. It should be pointed out that PAL is not soluble in epoxy EPO-TEK 301 as verified from a miscibility study. The epoxy bar containing the micrometer particles was microtomed. The thickness of the specimens was about 70 nm. Figure 3 shows that the particle size was about 10 nm, which should be the size of single molecules of the polymers employed.[23] Because the PAL sample had a wide molecular weight distribution, it is therefore seen, in Figure 3, that the particle sizes are not uniform.

Glass Transition and Chain Entanglement. Generally, the glassy state of amorphous polymers is not a true thermodynamic equilibrium state, because it consists of a series of nonequilibrium states due to chain entanglement and the slow relaxation of the chain segments.[24] It can be seen, as illustrated in Figure 4, that the change in the intensive variables, enthalpy H, entropy S, heat capacity C_p, and specific volume v, upon cooling exhibits a deviation from equilibrium at the

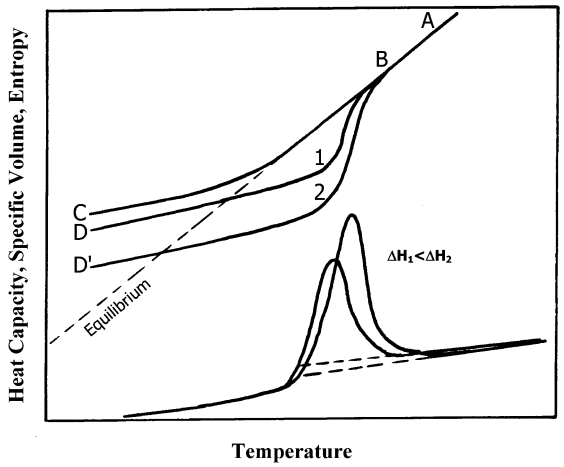

Figure 4. Change in the intensive thermodynamic variables before and after the glass transition temperature. The upper part of the figure demonstrates the change of specific volume or entropy as a function of temperature, and the lower part demonstrates the change of heat capacity as a function of temperature.

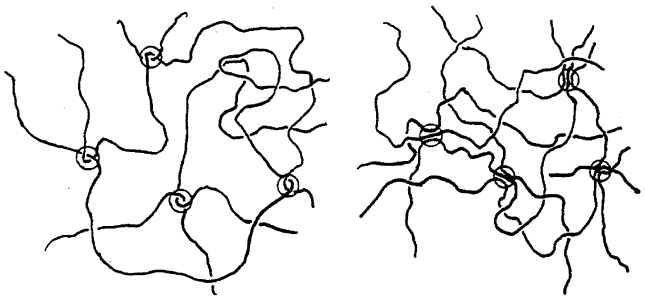

Figure 5. Illustration of the difference between topological and cohesional entanglements.

glass transition temperature (T_g). The upper part of Figure 4 demonstrates the change of volume or entropy as a function of temperature, and the lower part demonstrates the change of heat capacity as a function of temperature. More importantly, the curve behavior is rate dependent. Shown in Figure 4, AB represents the equilibrium heating and cooling curves for polymers in the rubbery state. At the glass transition, an inflection occurs and the curve becomes ABC. If the polymer is annealed near T_g, the heating curve will be DBA (curve 1). For even longer annealing, the heating curve behaves as D′BA (curve 2). Consequently, the DSC thermograms for curve 1 and curve 2 yield ΔH_1 and ΔH_2 and are also shown in Figure 4 in terms of the enthalpy relaxation peaks. It should be noted that, for the longer sub-T_g annealing, the enthalpy relaxation peak becomes higher and moves to the high-temperature end. Qian attributed the enthalpy relaxation peak to the cohesional entanglement in the polymer network.[25] The cohesional entanglement is formed due to a local nematic interaction between segments. Yet, this is different from the physical cross-linking of interlocked chain loops, which is defined as the topological entanglement. Figure 5 shows schematically the difference between topological and cohesional entanglements.

The topological entanglement of interlocked chain loops is characteristic of bulk polymers. When polymer molecules are in the isolated molecular state, such interlocking of the chain loops should not be great in the single-chain coils. The support of this viewpoint is Wu's experimental observation of the molten globule

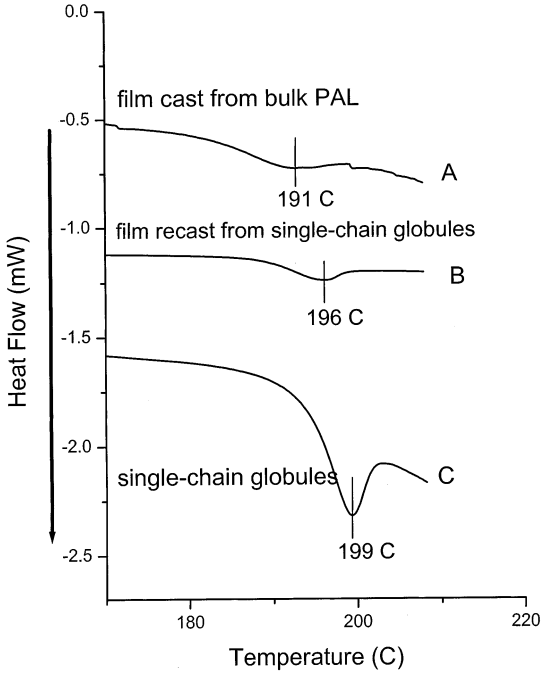

Figure 6. DSC thermograms for different PAL samples after annealing at 180 °C for 2 h: (A) film cast from bulk PAL, (B) film recast from single-chain globules, (C) single-chain globules.

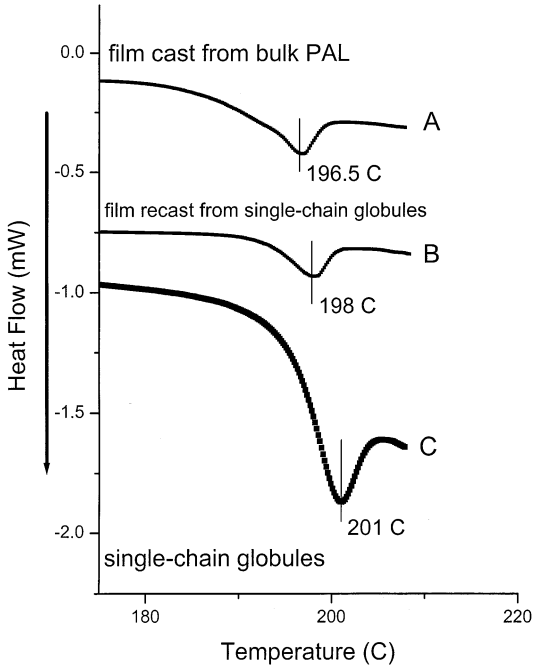

Figure 7. DSC thermograms for different PAL samples after annealing at 180 °C for 4 h: (A) film cast from bulk PAL, (B) film recast from single-chain globules, (C) single-chain globules.

state of a single homopolymer chain, in which the random coil of linear poly(*N*-isopropylacrylamide) was observed to clasp onto the single-chain globule when the solvent medium changed from a good solvent to a poor solvent.[26] Had there been many interlocks of chain loops in the single-chain coil, the clasp would not have happened as quickly as was observed within seconds.[26] When the topological entanglements are absent, the single-chain globules should possess more cohesional entanglements, as illustrated in Figure 5.[25]

Figure 6 shows the DSC thermograms of polyacrylamide in different states. All the samples in Figure 6 were annealed at 180 °C for 2 h. Curve A is the DSC thermogram of the bulk PAL, and curve C is that of the PAL single-chain globules. We also prepared DSC samples by dissolving the single-chain globules in water and cast a film for DSC study; hence, the DSC thermogram is shown as curve B in Figure 6. It can be seen that the bulk PAL exhibits a relatively small enthalpy relaxation peak at the glass transition (curve A) and the glass transition is also relatively broader. However, the single-chain globules exhibit both a higher glass transition and a higher enthalpy relaxation peak. For the film cast from the solution of redissolved single-chain globules, the glass transition and the enthalpy relaxation peak fell between those of the bulk and the single-chain globules (curve B). The concentration of PAL solution for spray-drying was 10^{-4} wt %, and the dissolution time was over one week. When we redissolved the single-chain globules, we prepared the solution with a concentration of 10% and dissolution time of about 5 min. Because the molecular weight of PAL is 5000000, the chain mixing, in a short period and at a high concentration, cannot be complete. Therefore, we believe that curve B actually illustrates the glass transition behavior for a partially entangled state.

Figure 7 shows the DSC thermograms for different PAL samples after annealing at 180 °C for 4 h, and the curve designation of A, B, and C in Figure 7 is the same

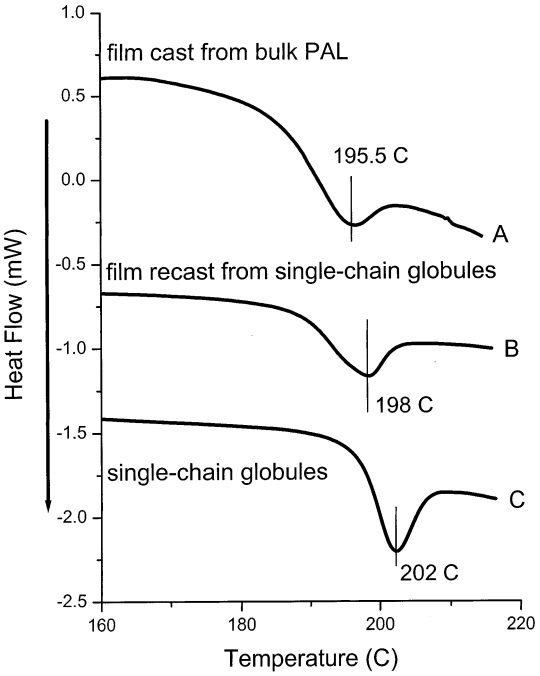

Figure 8. DSC thermograms for different PAL samples annealed at 190 °C and cooled at 0.5 °C/min: (A) film cast from bulk PAL, (B) film recast from single-chain globules, (C) single-chain globules.

as that in Figure 6. Comparing Figures 6 and 7, we find that, for longer annealing time, T_g moves to a higher temperature and the enthalpy relaxation peak becomes bigger and sharper. In Figures 6 and 7, the samples were subjected to cooling at a rate of 10 °C/min after annealing. Figure 8 shows, when the samples were annealed at 190 °C and cooled at 0.5 °C/min, the glass transition moved to an even higher temperature. However, it should be noted that Figures 6−8 only give the peak temperatures of the enthalpy relaxation peaks.

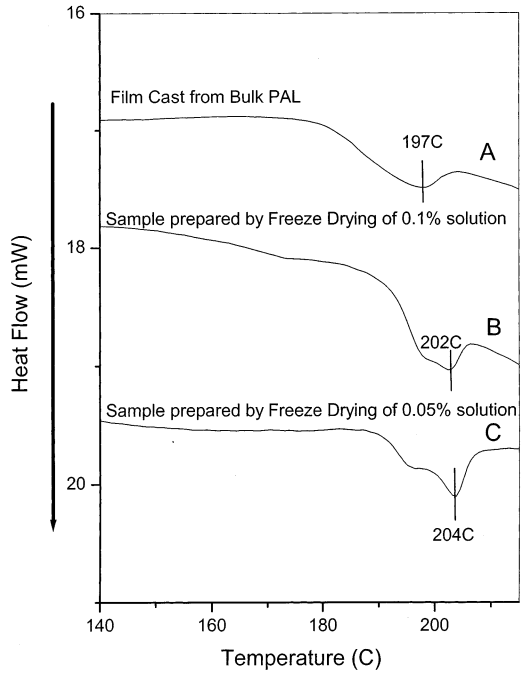

Figure 9. DSC thermograms of different PAL samples after annealing for 4 h at 180 °C: (A) film cast from bulk PAL, (B) PAL sample prepared by freeze-drying of 0.1% solution, (C) PAL sample prepared by freeze-drying of 0.05% solution.

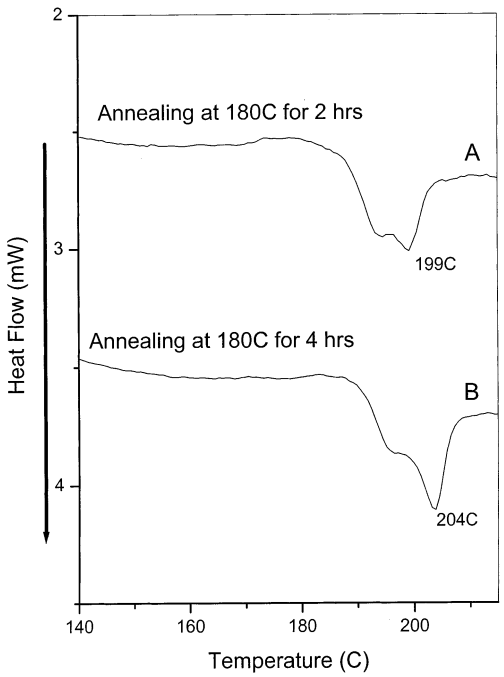

Figure 10. DSC thermograms of PAL samples prepared by freeze-drying of 0.05% solution with different annealing time: (A) annealing at 180 °C for 2 h, (B) annealing at 180 °C for 4 h.

The peak temperature should not be taken as the true glass transition temperature. Here, we only report and state two facts, namely (a) the glass transition phenomenon moves to higher temperature upon annealing and (b) at the same thermotreatment (annealing) condition, the glass transition phenomenon for single-chain globules occurs at higher temperature than that for the bulk polymer. Point a is common for all polymers; however, point b is a new observation of ours. To check the glass transition temperature without the effect of the enthalpy relaxation, we can treat the sample first by annealing at the temperature above the glass transition temperature and then by quenching. The results are presented in the next section.

Although curve B in Figures 6−8 is regarded as the glass transition phenomenon of PAL in the partially entangled state inferred by a logical speculation, it may not sound convincing enough. Besides, the PAL single-chain dissolution time and film-casting time cannot be controlled to be exactly the same for different samples since the casting procedure is by air-drying. To explore further the relationship between enthalpy relaxation and the chain entanglement, the low entangled PAL samples were prepared by the freeze-drying technique. Polymer coils are fully separated in the diluted solution when the concentration is much lower than the critical concentration c^*. If, however, the concentration is close to c^*, and polymer samples are obtained from sublimation of the frozen solution, a partially entangled sample could be obtained. Figure 9 shows three DSC thermograms, and the samples in Figure 9 were all annealed at 180 °C for 4 h. Curve A represents the glass transition phenomenon for the bulk PAL. Curve B represents the glass transition phenomenon for the PAL sample prepared by freeze-drying from 0.1% PAL solution. Curve C represents the glass transition phenomenon for the PAL sample prepared by freeze-drying from 0.05% PAL solution. It can be seen that there are two enthalpy relaxation peaks (or one peak and one shoulder) during the glass transition for the freeze-dried samples. If enthalpy relaxation can be explained by the cohesional entanglement theory as proposed by Qian,[25] we can explain curves B and C in Figure 9 by the following statement. For curves B and C in Figure 9, the peak that occurs at the higher temperature end represents the unentangled (or less entangled) mode in which the cohesional entanglements occur more easily. The shoulder represents the entangled (or relatively more entangled) mode in which cohesional entanglements are more prohibited by the interlocking of the chain loops.[25] This picture can be better comprehended by curve C, which represents the sample prepared by freeze-drying from 0.05% PAL solution. For the freeze-drying preparation, when the concentration is lower, the sample prepared should contain a larger chain population in the less entangled state and a smaller chain population in the entangled state. Considering the results shown in Figures 6−8, we feel that the two enthalpy relaxation peaks in Figure 9 can be attributed to the unentangled mode and the partially entangled mode, respectively. Consequently, the DSC result shows that, for curve C in Figure 9, the unentangled mode gives a stronger peak than the entangled mode, which appears as a shoulder. It is therefore concluded that, when PAL is in its single-chain state, in comparison to PAL in the bulk state, the glass transition temperature should move to higher temperature and the enthalpy relaxation peak should become stronger and sharper toward the high-temperature end. This is very well illustrated by the results in Figures 6−8.

It should also be noted that the chain conformations of PAL samples prepared either by spray-drying or by freeze-drying are not the same as the chain conformations in the equilibrium state. One should expect that the single-chain globules, although randomly coil-like, are in a more open and spread shape. Through annealing, the chain coils will approach a more equilibrium state. Figure 10 shows the DSC thermograms of the

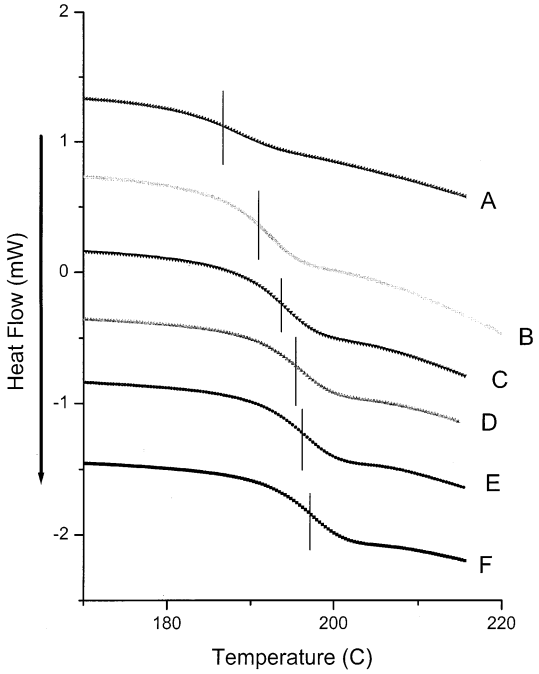

Figure 11. A series of DSC curves of the PAL single-chain samples prepared by spray-drying at a heating and cooling rate of 20 °C/min. Curve A is the first scan, B is the second scan, C is the third scan, D is the forth scan, E is the fifth scan, and F is the sixth scan.

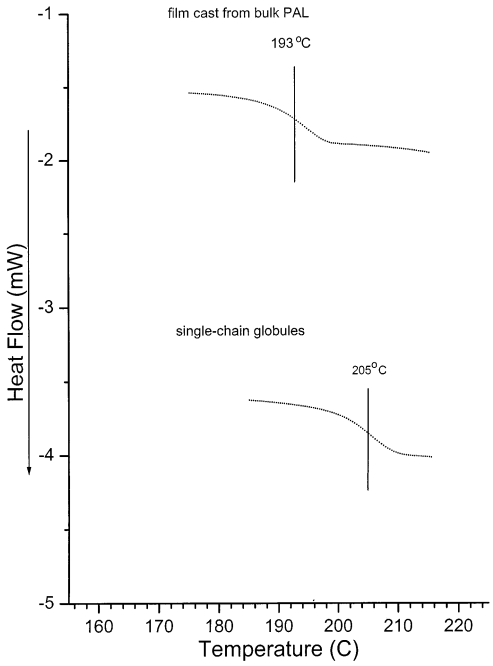

Figure 12. DSC thermograms of the bulk PAL sample and the single-chain PAL particles.

PAL sample prepared by freeze-drying from 0.05% solution. Curve A is the DSC result after the sample was annealed at 180 °C for 2 h, and curve B is that after the sample was annealed at 180 °C for 4 h. It can be seen that, for longer annealing, the unentangled single-chain mode is enhanced more as shown by the sharper and stronger peak at the high-temperature end in curve B in Figure 10. The enhancement in the enthalpy relaxation peak and the shift of the peak temperature to the higher temperature end could be attributed to self-aggregation of the unentangled chain population induced by annealing. This self-aggregation should also be related to the cohesional entanglement.

Figure 11 shows a series of DSC curves of the as-received PAL single-chain sample prepared by spray-drying without annealing at the heating and cooling rate of 20 °C/min. Curve A is the first scan of the DSC thermogram, B is the second scan, C is the third scan, D is the forth scan, E is the fifth scan, and F is the sixth scan. It can be seen that the glass transition temperature of the single-chain globules of PAL shifts, with increasing scan times, to the higher temperature end from about 188 to 198 °C. This result supports our suggestion that the single-chain coils transform from the initial more extended conformation to a more tightly coiled conformation upon annealing. The higher T_g suggests tighter globule coils are formed upon heating, and we believe this phenomenon is related to self-aggregation. When we took the bulk PAL sample as received from solution-casting without annealing treatment and did the DSC scans repeatedly seven times, the T_g remained invariant at 188 °C for the different scans.

Since Figures 6−10 involve enthalpy relaxation at the glass transition, the T_g values in these figures cannot be properly determined from the DSC thermograms. However, we can eliminate the enthalpy relaxation peak by annealing the sample at a temperature above T_g, quenching the sample, and then running DSC. Figure 12 shows the DSC thermograms which were preceded by annealing at 220 °C for 30 min and then quenching to 30 °C at a cooling rate of 100 °C/min. The T_g of the single-chain PAL particles is 205 °C, and that of the bulk PAL polymer is 193 °C. This again demonstrates that the T_g of the single-chain particles is higher than that of the bulk PAL samples.

Lastly, we remind the readers that there are some controversial reports in the single-chain study. Huang et al. reported, in their study, significant T_g reduction and concluded that T_g reduction was due to less entanglement of the single-chain molecules.[27,28] However, another report raised concerns about the sample preparation of Huang's paper and suspected that the residual solvent may be a factor for T_g reduction. After a reexamination, they reverted Huang's conclusion and said that the subtle T_g reduction of the freeze-drying sample cannot be attributed to less entanglement.[29] In this study, we did not observe any T_g reduction for the single-chain samples. On the contrary, we observed a significant T_g increase for the single-chain nanoglobules.

Conclusion

Single-chain globules of PAL, prepared by spray-drying, are in loose extended chain conformations. The loose conformation will be transformed into more tightly coiled single-chain globules upon heating. This transformation is supported by the higher T_g, as observed in this study, for the single-chain PAL globules than for the bulk PAL. TEM observation of the single-chian particles indicates that it does take some time for the single-chain nanoparticles to appear under the high-energy TEM electron beam. The perfect spherical conformation of PAL single molecules, observed in Figure 3, is very likely induced by the thermal energy of the TEM electron beam and is not likely the conformation of PAL single molecules right after the spray-drying. The enthalpy relaxation of the glass transition is described by the cohesional entanglement theory. It is

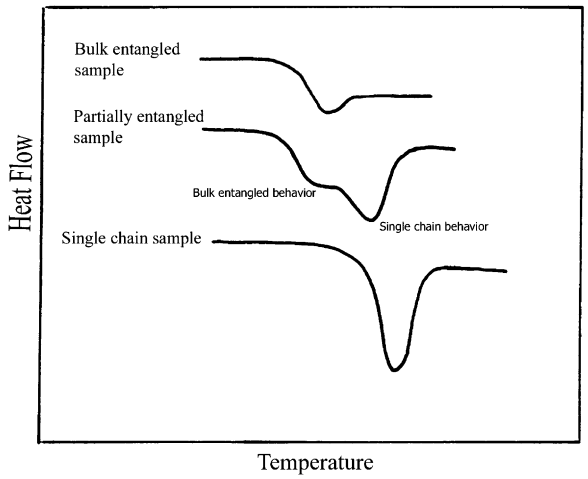

Figure 13. A schematic demonstration of the glass transition in three different modes.

believed that when polymer chains are in the less entangled state, self-aggregation may occur easily upon annealing. It appears that the theory agrees with our experimental observations. Figure 13 schematically demonstrates the glass transition in three different modes. The three modes are classified as a bulk entangled state, a partially entangled state, and an isolated single-chain state.

Acknowledgment. Financial support via an RGC Competitive Earmarked Research Grant, HKUST6195/01P, is gratefully acknowledged.

References and Notes

(1) Sokolov, A. P. *Science* **1996**, *273*, 1675.
(2) Beaucage, G.; Composto, R.; Stein, E. S. *J. Polym. Sci., Part B: Polym. Phys.* **1993**, *31*, 319.
(3) Orts, W. J.; van Zanten, J. H.; Wu, W. L.; Satija, S. K. *Phys. Rev. Lett.* **1993**, *71*, 867.
(4) van Zanten, J. H.; Wallace, W. E.; Wu, W. L. *Phys. Rev. E* **1996**, *53*, r2053.
(5) Wallace, W. E.; van Zanten, J. H.; Wu, W. L. *Phys. Rev. E* **1995**, *52*, r3329.
(6) Wu, W. L.; van Zanten, J. H.; Orts, W. J. *Macromolecules* **1995**, *28*, 771.
(7) Arndt, M.; Stannarius, R.; Groothues, H.; Hempel, E.; Kremer, F. *Phys. Rev. Lett.* **1997**, *79*, 2077.
(8) Keddie, J. L.; Jones, R. A. L.; Cory, R. A. *Europhys. Lett.* **1994**, *27*, 59.
(9) Forrest, J. A.; Dalnoki-Veress, K.; Stevens, J. R.; Dutcher, J. R. *Phys. Rev. Lett.* **1996**, *77*, 2002.
(10) Deppe, D. D.; Dhinojwala, A.; Torkelson, J. M. *Macromolecules* **1996**, *29*, 3898.
(11) Hall, D. B.; Hooker, J. C.; Torkelson, J. M. *Macromolecules* **1977**, *30*, 667.
(12) Fryer, D. S.; Nealey, P. F.; de Pablo, J. J. *Macromolecules* **2000**, *33*, 6439.
(13) Kerle, T.; Lin, Z.; Kim, H. C.; Russell, T. P. *Macromolecules* **2001**, *34*, 3484.
(14) Reiter, G. *Macromolecules* **1994**, *27*, 3046.
(15) Brown, H. R.; Russell, T. P. *Macromolecules* **1996**, *29*, 798.
(16) Tanaka, K.; Taura, A.; Ge, S. R.; Takahara, A.; Kajiyama, T. *Macromolecules* **1996**, *29*, 3040.
(17) Kajiyama, T.; Tanaka, K.; Takahara, A. *Macromolecules* **1997**, *30*, 280.
(18) de Gennes, P. G. *Eur. Phys. J.* **2000**, *E2*, 201.
(19) DeMaggio, G. B.; Frieze, W. E.; Gidley, D. W.; Zhu, M.; Hristov, H. A.; Yee, A. F. *Phys. Rev. Lett.* **1997**, *78*, 1524.
(20) Jean, Y. C.; Zhang, R.; Cao, H.; Yuan, J. P.; Hang, C. M.; Nielsen, B.; Asoka-Kumar, P. *Phys. Rev. B* **1997**, *56*, r8459.
(21) Douglas, J. F.; Ishinable, T. *Phys. Rev. E* **1995**, *51*, 1791.
(22) Mi, Y.; Xue, G.; Wang, X. *Polymer* **2002**, *43*, 6701.
(23) Mi, Y.; Wang, J.; Zhang, Y.; Chen, E.; Cheng, S. Z. D. *Polymer* **2001**, *42*, 4533.
(24) Keller, A.; Cheng, S. Z. D. *Polymer* **1998**, *39*, 4461.
(25) Qian, R. *Macromol. Symp.* **1997**, *124*, 15.
(26) Wu, C.; Zhou, S. *Phys. Rev. Lett.* **1996**, *77*, 3053.
(27) Huang, D.; Yang, Y.; Zhuang, G.; Li, B. *Macromolecules* **1999**, *32*, 6675.
(28) Huang, D.; Yang, Y.; Zhuang, G.; Li, B. *Macromolecules* **2000**, *33*, 461.
(29) Bernazzani, P.; Simon, S. L.; Plazek, D. J.; Ngai, K. L. *Eur. Phys. J. E* **2002**, *8*, 201.

MA030127J